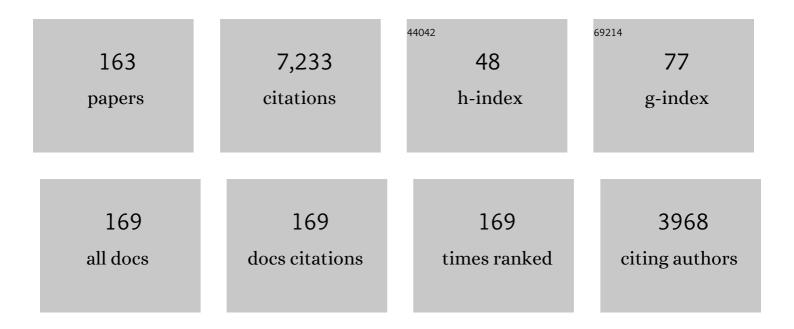
List of Publications by Year in descending order

Source: https://exaly.com/author-pdf/8735251/publications.pdf Version: 2024-02-01



ΥΠΝΖΗΙ ΜΑΝΟ

#	Article	IF	CITATIONS
1	A new αÂ+Âβ Ti-alloy with refined microstructures and enhanced mechanical properties in the as-cast state. Scripta Materialia, 2022, 207, 114260.	2.6	31
2	Role of point defects in the formation of relaxor ferroelectrics. Acta Materialia, 2022, 225, 117558.	3.8	20
3	Reentrant strain glass transition in Ti-Ni-Cu shape memory alloy. Acta Materialia, 2022, 226, 117618.	3.8	14
4	Quasiâ€Linear Superelasticity with Ultralow Modulus in Tensile Cyclic Deformed TiNi Strain Glass. Advanced Engineering Materials, 2022, 24, .	1.6	3
5	Pathways to Titanium Martensite. Transactions of the Indian Institute of Metals, 2022, 75, 1051-1068.	0.7	3
6	Strain Glass State, Strain Glass Transition, and Controlled Strain Release. Annual Review of Materials Research, 2022, 52, 159-187.	4.3	10
7	Strain states and unique properties in cold-rolled TiNi shape memory alloys. Acta Materialia, 2022, 231, 117890.	3.8	24
8	Exploration of spinodal decomposition in multi-principal element alloys (MPEAs) using CALPHAD modeling. Scripta Materialia, 2022, 214, 114657.	2.6	10
9	Solid solution strengthening of high-entropy alloys from first-principles study. Journal of Materials Science and Technology, 2022, 121, 105-116.	5.6	15
10	Existence of a quadruple point in a binary ferroelectric phase diagram. Physical Review B, 2021, 103, .	1.1	8
11	H-phase precipitation and its effects on martensitic transformation in NiTi-Hf high-temperature shape memory alloys. Acta Materialia, 2021, 208, 116651.	3.8	24
12	Influence of Ni4Ti3 precipitation on martensitic transformations in NiTi shape memory alloy: R phase transformation. Acta Materialia, 2021, 207, 116665.	3.8	40
13	Microstructure development and morphological transition during deposition of immiscible alloy films. Acta Materialia, 2021, 220, 117313.	3.8	10
14	Shearing mechanisms of co-precipitates in IN718. Acta Materialia, 2021, 220, 117305.	3.8	13
15	A general phase-field framework for predicting the structures and micromechanical properties of crystalline defects. Materials and Design, 2021, 209, 109959.	3.3	2
16	Phase field simulation of the stress-induced α microstructure in Ti–6Al–4ÂV alloy and its CPFEM properties evaluation. Journal of Materials Science and Technology, 2021, 90, 168-182.	5.6	19
17	Achieving large super-elasticity through changing relative easiness of deformation modes in Ti-Nb-Mo alloy by ultra-grain refinement. Materials Research Letters, 2021, 9, 223-230.	4.1	11
18	Harmonic Noise-Elimination Method Based on the Synchroextracting Transform for Magnetic-Resonance Sounding Data. IEEE Transactions on Instrumentation and Measurement, 2021, 70, 1-11.	2.4	8

#	Article	IF	CITATIONS
19	Stress-dependent dislocation core structures leading to non-Schmid behavior. Materials Research Letters, 2021, 9, 134-140.	4.1	9
20	High temperature phase stability of the compositionally complex alloy AlMo0.5NbTa0.5TiZr. Applied Physics Letters, 2021, 119, .	1.5	14
21	In situ design of advanced titanium alloy with concentration modulations by additive manufacturing. Science, 2021, 374, 478-482.	6.0	168
22	Phase-field modelling of transformation pathways and microstructural evolution in multi-principal element alloys. Applied Physics Letters, 2021, 119, .	1.5	17
23	Creep Behavior of Compact γ′-γ″ Coprecipitation Strengthened IN718-Variant Superalloy. Metals, 2021, 11, 1897.	1.0	3
24	Medium-range ordering, structural heterogeneity, and their influence on properties of Zr-Cu-Co-Al metallic glasses. Physical Review Materials, 2021, 5, .	0.9	8
25	Generalized stacking fault energy surface mismatch and dislocation transformation. Npj Computational Materials, 2021, 7, .	3.5	6
26	The role of nano-scaled structural non-uniformities on deformation twinning and stress-induced transformation in a cold rolled multifunctional β-titanium alloy. Scripta Materialia, 2020, 177, 181-185.	2.6	45
27	Shuffle-nanodomain regulated strain glass transition in Ti-24Nb-4Zr-8Sn alloy. Acta Materialia, 2020, 186, 415-424.	3.8	52
28	Linear-superelastic metals by controlled strain release via nanoscale concentration-gradient engineering. Materials Today, 2020, 33, 17-23.	8.3	33
29	Generalized Stacking Fault Energy of Al-Doped CrMnFeCoNi High-Entropy Alloy. Nanomaterials, 2020, 10, 59.	1.9	37
30	Intrinsic coupling between twinning plasticity and transformation plasticity in metastable β Ti-alloys: A symmetry and pathway analysis. Acta Materialia, 2020, 196, 488-504.	3.8	24
31	Polarization Spinodal at Ferroelectric Morphotropic Phase Boundary. Physical Review Letters, 2020, 125, 127602.	2.9	14
32	Critical nuclei at hetero-phase interfaces. Acta Materialia, 2020, 200, 510-525.	3.8	11
33	Revealing the atomistic mechanisms of strain glass transition in ferroelastics. Acta Materialia, 2020, 194, 134-143.	3.8	14
34	Determination of twinning path from broken symmetry: A revisit to deformation twinning in bcc metals. Acta Materialia, 2020, 196, 280-294.	3.8	23
35	Novel transformation pathway and heterogeneous precipitate microstructure in Ti-alloys. Acta Materialia, 2020, 196, 409-417.	3.8	35
36	Phase Transformation Graph and Transformation Pathway Engineering for Shape Memory Alloys. Shape Memory and Superelasticity, 2020, 6, 115-130.	1.1	7

#	Article	IF	CITATIONS
37	Non-conventional transformation pathways and ultrafine lamellar structures in Î ³ -TiAl alloys. Acta Materialia, 2020, 189, 25-34.	3.8	34
38	Finite strain phase-field microelasticity theory for modeling microstructural evolution. Acta Materialia, 2020, 191, 253-269.	3.8	17
39	Defect-free plastic deformation through dimensionality reduction and self-annihilation of topological defects in crystalline solids. Physical Review Research, 2020, 2, .	1.3	1
40	Ϊ‰-Assisted Î \pm nucleation in a metastable Î 2 titanium alloy. Scripta Materialia, 2019, 171, 62-66.	2.6	41
41	Structure, Morphology and Coarsening Behavior of MX (NbC) Nanoprecipitates in Fe-Ni-Cr Based Alloys. Microscopy and Microanalysis, 2019, 25, 2612-2613.	0.2	0
42	Dissecting the influence of nanoscale concentration modulation on martensitic transformation in multifunctional alloys. Acta Materialia, 2019, 181, 99-109.	3.8	10
43	Making metals linear super-elastic with ultralow modulus and nearly zero hysteresis. Materials Horizons, 2019, 6, 515-523.	6.4	27
44	On the use of metastable interface equilibrium assumptions on prediction of solidification micro-segregation in laser powder bed fusion. Science and Technology of Welding and Joining, 2019, 24, 446-456.	1.5	5
45	Slip transmission assisted by Shockley partials across <mml:math xmlns:mml="http://www.w3.org/1998/Math/MathML" altimg="si1.gif" overflow="scroll"><mml:mrow><mml:mi>α</mml:mi><mml:mo>/</mml:mo><mml:mi>β</mml:mi> interfaces in Ti-alloys. Acta Materialia. 2019. 171. 291-305.</mml:mrow></mml:math 	row><१mml:ı	nath>
46	Microstructural design for advanced light metals. MRS Bulletin, 2019, 44, 281-286.	1.7	4
47	Tilt strain glass in Sr and Nb co-doped LaAlO3 ceramics. Acta Materialia, 2019, 168, 250-260.	3.8	12
48	Nano-scale structural non-uniformities in gum like Ti-24Nb-4Zr-8Sn metastable β-Ti alloy. Scripta Materialia, 2019, 158, 95-99.	2.6	45
49	Predicting grain boundary structure and energy in BCC metals by integrated atomistic and phase-field modeling. Acta Materialia, 2019, 164, 799-809.	3.8	22
50	Growth behavior of <mml:math <br="" altimg="si1.gif" xmlns:mml="http://www.w3.org/1998/Math/MathML">overflow="scroll"><mml:mrow><mml:mi>l³</mml:mi><mml:mo>'</mml:mo><mml:mo>/</mml:mo><mml:mi coprecipitates in Ni-Base superalloys. Acta Materialia, 2019, 164, 220-236.</mml:mi </mml:mrow></mml:math>	>Î ³ 3n8l:mi	> <rā#nl:mo>'<</r
51	Phase field simulation of martensitic transformation in pre-strained nanocomposite shape memory alloys. Acta Materialia, 2019, 164, 99-109.	3.8	32
52	Deformation pathway and defect generation in crystals: a combined group theory and graph theory description. IUCrJ, 2019, 6, 96-104.	1.0	12
53	Development of low-alloyed and rare-earth-free magnesium alloys having ultra-high strength. Acta Materialia, 2018, 149, 350-363.	3.8	287
54	Interaction of Trace Rareâ€Earth Dopants and Nanoheterogeneities Induces Giant Magnetostriction in Feâ€Ga Alloys. Advanced Functional Materials, 2018, 28, 1800858.	7.8	64

#	Article	IF	CITATIONS
55	Form of critical nuclei at homo-phase boundaries. Scripta Materialia, 2018, 146, 276-280.	2.6	12
56	Enabling Large Superalloy Parts Using Compact Coprecipitation of γâ€2 and Î3â€2â€2. Metallurgical and Materials Transactions A: Physical Metallurgy and Materials Science, 2018, 49, 708-717.	1.1	53
57	Microstructural and micromechanical evolution during dynamic recrystallization. International Journal of Plasticity, 2018, 100, 52-68.	4.1	66
58	Probing Nanoscale Structural Heterogeneity in Metallic Glasses Using 4-D STEM. Microscopy and Microanalysis, 2018, 24, 202-203.	0.2	1
59	Phase Field Model and Computer Simulation of Strain Glasses. Springer Series in Materials Science, 2018, , 253-272.	0.4	Ο
60	Direct determination of structural heterogeneity in metallic glasses using four-dimensional scanning transmission electron microscopy. Ultramicroscopy, 2018, 195, 189-193.	0.8	44
61	Shearing of γ' particles in Co-base and Co-Ni-base superalloys. Acta Materialia, 2018, 161, 99-109.	3.8	45
62	Heterogeneous <mml:math <br="" altimg="si1.gif" xmlns:mml="http://www.w3.org/1998/Math/MathML">overflow="scroll"><mml:mtext>γâ€2</mml:mtext></mml:math> microstructures in nickel-base superalloys and their influence on tensile and creep performance. International Journal of Plasticity, 2018, 109, 153-168.	4.1	12
63	A homogenized primary creep model of nickel-base superalloys and its application to determining micro-mechanistic characteristics. International Journal of Plasticity, 2018, 110, 202-219.	4.1	15
64	Phase Formation in Ti–Ni Binary System during Solid-State Synthesis. Shape Memory and Superelasticity, 2018, 4, 351-359.	1.1	4
65	Three-dimensional phase field simulation of intragranular void formation and thermal conductivity in irradiated α-Fe. Journal of Materials Science, 2018, 53, 11002-11014.	1.7	15
66	Cubic martensite in high carbon steel. Physical Review Materials, 2018, 2, .	0.9	4
67	Self-organized multigrain patterning with special grain boundaries produced by phase transformation cycling. Physical Review Materials, 2018, 2, .	0.9	13
68	Hidden pathway during fcc to bcc/bct transformations: Crystallographic origin of slip martensite in steels. Physical Review Materials, 2018, 2, .	0.9	7
69	Giant strain with low hysteresis in A-site-deficient (Bi0.5Na0.5)TiO3-based lead-free piezoceramics. Acta Materialia, 2017, 128, 337-344.	3.8	222
70	A universal symmetry criterion for the design of high performance ferroic materials. Acta Materialia, 2017, 127, 438-449.	3.8	42
71	Monte Carlo simulation of magnetic domain structure and magnetic properties near the morphotropic phase boundary. Physical Chemistry Chemical Physics, 2017, 19, 7236-7244.	1.3	5
72	Influence of nanoscale structural heterogeneity on shear banding in metallic glasses. Acta Materialia, 2017, 134, 104-115.	3.8	42

#	Article	IF	CITATIONS
73	Taming martensitic transformation via concentration modulation at nanoscale. Acta Materialia, 2017, 130, 196-207.	3.8	52
74	Mechanical behavior and microstructural analysis of NiTi-40Au shape memory alloys exhibiting work output above 400°C. Intermetallics, 2017, 86, 33-44.	1.8	27
75	Ferroic glasses. Npj Computational Materials, 2017, 3, .	3.5	27
76	Origin of the modulus anomaly over a wide temperature range of Mn0.70Fe0.25Cu0.05 alloy. Computational Materials Science, 2017, 140, 89-94.	1.4	3
77	Large electrocaloric efficiency over a broad temperature span in lead-free BaTiO3-based ceramics near room temperature. Applied Physics Letters, 2017, 111, .	1.5	27
78	Effect of nonlinear and noncollinear transformation strain pathways in phase-field modeling of nucleation and growth during martensite transformation. Npj Computational Materials, 2017, 3, .	3.5	13
79	Crystallographic analysis and phase field simulation of transformation plasticity in a multifunctional β-Ti alloy. International Journal of Plasticity, 2017, 89, 110-129.	4.1	31
80	Simulation Study of Heterogeneous Nucleation at Grain Boundaries During the Austenite-Ferrite Phase Transformation: Comparing the Classical Model with the Multi-Phase Field Nudged Elastic Band Method. Metallurgical and Materials Transactions A: Physical Metallurgy and Materials Science, 2017, 48, 2730-2738.	1.1	18
81	Novel B19â \in ² strain glass with large recoverable strain. Physical Review Materials, 2017, 1, .	0.9	20
82	New Insights into Deformation of Metallic Glasses by Combining Mesoscale Simulation and Fluctuation Electron Microscopy. Microscopy and Microanalysis, 2016, 22, 1436-1437.	0.2	1
83	Accelerating ferroic ageing dynamics upon cooling. NPG Asia Materials, 2016, 8, e319-e319.	3.8	7
84	Novel Characterization of Deformation Mechanisms in a Ni-base Superalloy Using HAADF Imaging and Atomic Ordering Analysis. Microscopy and Microanalysis, 2016, 22, 272-273.	0.2	2
85	Quantification of rafting of γ′ precipitates in Ni-based superalloys. Acta Materialia, 2016, 103, 322-333.	3.8	46
86	Defect strength and strain glass state in ferroelastic systems. Journal of Alloys and Compounds, 2016, 661, 100-109.	2.8	31
87	Effect of low-angle grain boundaries on morphology and variant selection of grain boundary allotriomorphs and WidmanstÄtten side-plates. Acta Materialia, 2016, 112, 347-360.	3.8	47
88	Deformation mechanisms of D022 ordered intermetallic phase in superalloys. Acta Materialia, 2016, 118, 350-361.	3.8	41
89	Effect of autocatalysis on variant selection of α precipitates during phase transformation in Ti-6Al-4V alloy. Computational Materials Science, 2016, 124, 282-289.	1.4	33
90	An integrated full-field model of concurrent plastic deformation and microstructure evolution: Application to 3D simulation of dynamic recrystallization in polycrystalline copper. International Journal of Plasticity, 2016, 80, 38-55.	4.1	89

#	Article	IF	CITATIONS
91	On variant distribution and coarsening behavior of the α phase in a metastable β titanium alloy. Acta Materialia, 2016, 106, 374-387.	3.8	98
92	Group theory description of transformation pathway degeneracy in structural phase transformations. Acta Materialia, 2016, 109, 353-363.	3.8	49
93	Role of ω phase in the formation of extremely refined intragranular α precipitates in metastable β-titanium alloys. Acta Materialia, 2016, 103, 850-858.	3.8	201
94	The indirect influence of the ω phase on the degree of refinement of distributions of the α phase in metastable β-Titanium alloys. Acta Materialia, 2016, 103, 165-173.	3.8	111
95	The role of the ω phase on the non-classical precipitation of the α phase in metastable β-titanium alloys. Scripta Materialia, 2016, 111, 81-84.	2.6	93
96	Modeling and Simulation of Microstructure Evolution during Heat Treatment of Titanium Alloys. , 2016, , 573-603.		3
97	A new mechanism for low and temperature-independent elastic modulus. Scientific Reports, 2015, 5, 11477.	1.6	33
98	A biopolymer-like metal enabled hybrid material with exceptional mechanical prowess. Scientific Reports, 2015, 5, 8357.	1.6	23
99	Effect of external stress on \hat{I}^3 nucleation and evolution in TiAl alloys. Intermetallics, 2015, 65, 1-9.	1.8	11
100	Quantifying the abnormal strain state in ferroelastic materials: A moment invariant approach. Acta Materialia, 2015, 94, 172-180.	3.8	8
101	Microstructure and transformation texture evolution during α precipitation in polycrystalline α/β titanium alloys – A simulation study. Acta Materialia, 2015, 94, 224-243.	3.8	41
102	Phase-Field Simulation of Orowan Strengthening by Coherent Precipitate Plates in an Aluminum Alloy. Metallurgical and Materials Transactions A: Physical Metallurgy and Materials Science, 2015, 46, 3287-3301.	1.1	41
103	Phase Field Simulation of Orowan Strengthening by Coherent Precipitate Plates in a Mg-Nd Alloy. , 2015, , 63-71.		3
104	Pattern formation during cubic to orthorhombic martensitic transformations in shape memory alloys. Acta Materialia, 2014, 68, 93-105.	3.8	42
105	Superelasticity of slim hysteresis over a wide temperature range by nanodomains of martensite. Acta Materialia, 2014, 66, 349-359.	3.8	81
106	Extended defects, ideal strength and actual strengths of finite-sized metallic glasses. Acta Materialia, 2014, 73, 149-166.	3.8	31
107	High-energy X-ray diffuse scattering studies on deformation-induced spatially confined martensitic transformations in multifunctional Ti–24Nb–4Zr–8Sn alloy. Acta Materialia, 2014, 81, 476-486.	3.8	29
108	Integrated Computational Materials Engineering (ICME) Approach to Design of Novel Microstructures for Ti-Alloys. Jom, 2014, 66, 1287-1298.	0.9	27

#	Article	IF	CITATIONS
109	A simulation study of β 1 precipitation on dislocations in an Mg–rare earth alloy. Acta Materialia, 2014, 77, 133-150.	3.8	60
110	Predicting structure and energy of dislocations and grain boundaries. Acta Materialia, 2014, 74, 125-131.	3.8	54
111	Variant selection of grain boundary α by special prior β grain boundaries in titanium alloys. Acta Materialia, 2014, 75, 156-166.	3.8	142
112	Strain glass transition in a multifunctional \hat{l}^2 -type Ti alloy. Scientific Reports, 2014, 4, 3995.	1.6	76
113	Unique properties associated with normal martensitic transition and strain glass transition – A simulation study. Journal of Alloys and Compounds, 2013, 577, S102-S106.	2.8	4
114	Variant selection during α precipitation in Ti–6Al–4V under the influence of local stress – A simulation study. Acta Materialia, 2013, 61, 6006-6024.	3.8	129
115	Heterogeneously randomized STZ model of metallic glasses: Softening and extreme value statistics during deformation. International Journal of Plasticity, 2013, 40, 1-22.	4.1	78
116	Formation mechanisms of self-organized core/shell and core/shell/corona microstructures in liquid droplets of immiscible alloys. Acta Materialia, 2013, 61, 1229-1243.	3.8	122
117	Numerical simulation of irradiation hardening in Zirconium. Journal of Nuclear Materials, 2013, 438, 209-217.	1.3	18
118	New intrinsic mechanism on gum-like superelasticity of multifunctional alloys. Scientific Reports, 2013, 3, 2156.	1.6	57
119	3D PHASE FIELD SIMULATION OF EFFECT OF INTERFACIAL ENERGY ANISOTROPY ON SIDEPLATE GROWTH IN Ti6Al4V. Jinshu Xuebao/Acta Metallurgica Sinica, 2013, 48, 148-158.	0.3	5
120	Finding activation pathway of coupled displacive-diffusional defect processes in atomistics: Dislocation climb in fcc copper. Physical Review B, 2012, 86, .	1.1	25
121	Microstructure Map for Self-Organized Phase Separation during Film Deposition. Physical Review Letters, 2012, 109, 086101.	2.9	49
122	Phase diagram of polar states in doped ferroelectric systems. Physical Review B, 2012, 86, .	1.1	52
123	Simulation study of precipitation in an Mg–Y–Nd alloy. Acta Materialia, 2012, 60, 4819-4832.	3.8	84
124	Quantifying microstructures in isotropic grain growth from phase field modeling: Methods. Acta Materialia, 2012, 60, 4787-4799.	3.8	10
125	Phase-field simulation of twin boundary fractions in fully lamellar TiAl alloys. Acta Materialia, 2012, 60, 6372-6381.	3.8	28
126	P-phase precipitation and its effect on martensitic transformation in (Ni,Pt)Ti shape memory alloys. Acta Materialia, 2012, 60, 1514-1527.	3.8	50

#	Article	IF	CITATIONS
127	Coupling Microstructure Characterization with Microstructure Evolution. , 2011, , 151-197.		ο
128	Diffusive molecular dynamics and its application to nanoindentation and sintering. Physical Review B, 2011, 84, .	1.1	67
129	Modeling displacive–diffusional coupled dislocation shearing of γ′ precipitates in Ni-base superalloys. Acta Materialia, 2011, 59, 3484-3497.	3.8	57
130	Strain glass in Fe-doped Ti–Ni. Acta Materialia, 2010, 58, 6206-6215.	3.8	152
131	Effect of Ni4Ti3 precipitation on martensitic transformation in Ti–Ni. Acta Materialia, 2010, 58, 6685-6694.	3.8	140
132	Phase field modeling of defects and deformation. Acta Materialia, 2010, 58, 1212-1235.	3.8	365
133	Modeling Abnormal Strain States in Ferroelastic Systems: The Role of Point Defects. Physical Review Letters, 2010, 105, 205702.	2.9	128
134	Large-scale three-dimensional phase field simulation of γ ′-rafting and creep deformation. Philosophical Magazine, 2010, 90, 405-436.	0.7	98
135	Phase-Field Microstructure Modeling. , 2009, , 297-311.		5
136	Phase Field Modeling of Microstructural Evolution in Solids: Effect of Coupling among Different Extended Defects. Metallurgical and Materials Transactions A: Physical Metallurgy and Materials Science, 2008, 39, 1630-1637.	1.1	8
137	Finding Critical Nucleus in Solid-State Transformations. Metallurgical and Materials Transactions A: Physical Metallurgy and Materials Science, 2008, 39, 976-983.	1.1	46
138	Systematic Approach to Microstructure Design of Ni-Base Alloys Using Classical Nucleation and Growth Relations Coupled with Phase Field Modeling. Metallurgical and Materials Transactions A: Physical Metallurgy and Materials Science, 2008, 39, 984-993.	1.1	12
139	Effect of elastic interaction on nucleation: II. Implementation of strain energy of nucleus formation in the phase field method. Acta Materialia, 2007, 55, 1457-1466.	3.8	89
140	Phase field modeling of channel dislocation activity and γ′ rafting in single crystal Ni–Al. Acta Materialia, 2007, 55, 5369-5381.	3.8	88
141	Effect of elastic interaction on nucleation: I. Calculation of the strain energy of nucleus formation in an elastically anisotropic crystal of arbitrary microstructure. Acta Materialia, 2006, 54, 5617-5630.	3.8	67
142	Multi-scale phase field approach to martensitic transformations. Materials Science & Engineering A: Structural Materials: Properties, Microstructure and Processing, 2006, 438-440, 55-63.	2.6	69
143	Implementation of high interfacial energy anisotropy in phase field simulations. Scripta Materialia, 2006, 54, 1919-1924.	2.6	25
144	Quantitative phase field modeling of diffusion-controlled precipitate growth and dissolution in Ti–Al–V. Scripta Materialia, 2004, 50, 471-476.	2.6	153

#	Article	IF	CITATIONS
145	Incorporation of Î ³ -surface to phase field model of dislocations: simulating dislocation dissociation in fcc crystals. Acta Materialia, 2004, 52, 683-691.	3.8	142
146	Movement of Kirkendall markers, second phase particles and the Type 0 boundary in two-phase diffusion couple simulations. Acta Materialia, 2004, 52, 1917-1925.	3.8	27
147	Solute segregation transition and drag force on grain boundaries. Acta Materialia, 2003, 51, 3687-3700.	3.8	57
148	Phase field model of dislocation networks. Acta Materialia, 2003, 51, 2595-2610.	3.8	127
149	Modeling Dislocation Dissociation and Cutting of γ′ Precipitates in Ni-Based Superalloys by the Phase Field Method. Materials Research Society Symposia Proceedings, 2002, 753, 1.	0.1	3
150	Grain growth in anisotropic systems: comparison of effects of energy and mobility. Acta Materialia, 2002, 50, 2491-2502.	3.8	161
151	A phase field study of microstructural changes due to the Kirkendall effect in two-phase diffusion couples. Acta Materialia, 2001, 49, 3401-3408.	3.8	63
152	Simulating Microstructural Evolution and Electrical Transport in Ceramic Gas Sensors. Journal of the American Ceramic Society, 2000, 83, 2219-2226.	1.9	39
153	Numerical Calculation of Electrical Conductivity of Porous Electroceramics. , 1999, 3, 17-23.		10
154	Indirect nucleation in phase transformations with symmetry reduction. Philosophical Magazine A: Physics of Condensed Matter, Structure, Defects and Mechanical Properties, 1996, 74, 1407-1420.	0.7	7
155	Modeling of Dynamical Evolution of Micro/Mesoscopic Morphological Patterns in Coherent Phase Transformations. , 1996, , 325-371.		16
156	Microstructural Development of Coherent Tetragonal Precipitates in Magnesium-Partially-Stabilized Zirconia: A Computer Simulation. Journal of the American Ceramic Society, 1995, 78, 657-661.	1.9	86
157	Microstructural evolution during the precipitation of ordered intermetallics in multiparticle coherent systems. Philosophical Magazine A: Physics of Condensed Matter, Structure, Defects and Mechanical Properties, 1995, 72, 1161-1171.	0.7	29
158	Shape Evolution of a Coherent Tetragonal Precipitate in Partially Stabilized Cubic ZrO2: A Computer Simulation. Journal of the American Ceramic Society, 1993, 76, 3029-3033.	1.9	57
159	Particle translational motion and reverse coarsening phenomena in multiparticle systems induced by a long-range elastic interaction. Physical Review B, 1992, 46, 11194-11197.	1.1	41
160	Kinetics of tweed and twin formation during an ordering transition in a substitutional solid solution. Philosophical Magazine Letters, 1992, 65, 15-23.	0.5	93
161	Shape evolution of a precipitate during strain-induced coarsening. Scripta Metallurgica Et Materialia, 1991, 25, 1387-1392.	1.0	74
162	Transformation-induced elastic strain effect on the precipitation kinetics of ordered intermetallics. Philosophical Magazine Letters, 1991, 64, 241-251.	0.5	62

#	Article	IF	CITATIONS
163	$\hat{I}\pm$ phase growth and branching in titanium alloys. Philosophical Magazine, 0, , 1-24.	0.7	1